Uncertainties in assessing tillage erosion – How appropriate are our measuring techniques?

Fiener P. [a,*], Wilken F. [a,b], Aldana-Jague E. [c], Deumlich D. [b], Gómez J.A. [d], Guzmán G. [d], Hardy R.A. [e], Quinton J.N. [e], Sommer M. [b,f], Van Oost K. [c], Wexler R. [a]

[a] Institute of Geography, University Augsburg, Augsburg, Germany
[b] Institute of Soil Landscape Research, Leibniz-Centre for Agricultural Landscape Research ZALF e.V., Müncheberg, Germany
[c] Georges Lemaître Centre for Earth and Climate Research (TECLIM), Université Catholique de Louvain, Louvain-la-Neuve, Belgium
[d] Institute for Sustainable Agriculture, Spanish National Research Council, Department of Agronomy, Córdoba, Spain
[e] Lancaster Environment Centre, Lancaster University, Lancaster, UK
[f] Institute of Earth and Environmental Sciences, University of Potsdam, Germany

Keywords:
Tillage erosion
Tracer
UAS
TLS
Method comparison
Measurement uncertainty

A B S T R A C T

Tillage erosion on arable land is a very important process leading to a net downslope movement of soil and soil constitutes. Tillage erosion rates are commonly in the same order of magnitude as water erosion rates and can be even higher, especially under highly mechanized agricultural soil management. Despite its prevalence and magnitude, tillage erosion is still understudied compared to water erosion. The goal of this study was to bring together experts using different techniques to determine tillage erosion and use the different results to discuss and quantify uncertainties associated with tillage erosion measurements. The study was performed in northeastern Germany on a 10 m by 50 m plot with a mean slope of 8%. Tillage erosion was determined after two sequences of seven tillage operations. Two different micro-tracers (magnetic iron oxide mixed with soil and fluorescent sand) and one macro-tracer (passive radio-frequency identification transponders (RFIDs), size: 4×22 mm) were used to directly determine soil fluxes. Moreover, tillage induced changes in topography were measured for the entire plot with two different terrestrial laser scanners and an unmanned aerial system for structure from motion topography analysis. Based on these elevation differences, corresponding soil fluxes were calculated. The mean translocation distance of all techniques was 0.57 m per tillage pass, with a relatively wide range of mean soil translocation distances ranging from 0.39 to 0.72 m per pass. A benchmark technique could not be identified as all used techniques have individual error sources, which could not be quantified. However, the translocation distances of the macro-tracers used were consistently smaller than the translocation distances of the micro-tracers (mean difference $= -26 \pm 12\%$), which questions the widely used assumption of non-selective soil transport via tillage operations. This study points out that tillage erosion measurements, carried out under almost optimal conditions, are subject to major uncertainties that are far from negligible.

1. Introduction

Soil erosion, especially on arable land, is a major environmental threat (Pimentel, 2006; Montanarella et al., 2016) negatively affecting on-site soil properties and leading to substantial off-site damage (Pimentel and Burgess, 2013). Moreover, lateral soil fluxes due to soil erosion are important modulators of biogeochemical cycles within soils (Quinton et al., 2010; Doetterl et al., 2016) and also substantially affect carbon and nutrient cycling in inland waters (Battin et al., 2009; Tranvik et al., 2009). Soil erosion is most commonly understood as a process driven by water and wind that redistributes soil within the terrestrial environment and transfers it to water courses. However, since the early 1990s there has been a growing awareness of tillage as another important agent of soil erosion and redistribution (Lindstrom et al., 1990; Govers et al., 1993; Lobb et al., 1995). Tillage on sloping land leads to a net downslope displacement of soil, even if upslope and downslope tillage directions are alternated (Govers et al., 1999). The major difference between tillage and water or wind erosion is: (i) that tillage erosion occurs on a regular basis and is not driven by rare extreme events; and (ii) that soil is redistributed entirely within fields and hence the process does not lead to off-site damage. Tillage erosion typically occurs on convex slopes while soil accumulation takes place in concavities (Govers et al., 1999). Hence, tillage and water erosion tends to take place at different landscape positions: tillage mobilizes soil from hilltops that are minimally affected by water erosion

* Corresponding author at: Alter Postweg 118, D-86159 Augsburg, Germany.
E-mail address: fiener@geo.uni-augsburg.de (P. Fiener).

to the thalwegs where the highest rates of water erosion occur (Govers et al., 1994).

Various authors have shown that tillage erosion rates on arable land are at least in the same order of magnitude as water erosion rates (Li et al., 1999; Van Oost et al., 2006) and might be even higher than water erosion rates in drier or less convective storm dominated areas (Sommer et al., 2008). Despite its prevalence and magnitude, tillage erosion is still understudied compared to water erosion: a Web-of-Knowledge search for articles including the topic 'water erosion' or 'tillage erosion' resulted in roughly ten times more results for 'water erosion' (260 vs. 2222; May 2017).

There are a variety of techniques presented in the literature for determining tillage erosion rates. These can be categorized as either tracer-based or those that determine topographic change or directly determine the movement of soil. For tracing methods, tracers are either added before performing individual or a series of tillage operations, or in-situ tracers (e.g., ^{137}Cs, Van Oost et al., 2006) are used to estimate long-term (decades to centuries) erosion rates. Tracers added before tillage experiments have the advantage that tillage erosion can be isolated from long-term erosion, which is always a combination of different erosion processes. The added tracers can be subdivided into macro-tracers (diameter > 2 mm) and micro-tracers (<2 mm diameter; subsequently this size-related micro- and macro-tracer definition is used). Micro-tracers are applied as solutes sprayed onto soil, e.g., sodium chloride solution (Barneveld et al., 2009), or mixed with natural soil and applied in trenches within the experimental plots, e.g., magnetic particles (Zhang and Li, 2011) or chloride (often as KCL) (Lobb et al., 1999). The recovery of the tracer after the experiment is either performed via soil sampling and/or if possible (e.g., in case of magnetic tracers) with instruments measuring in-situ concentrations as used by Guzmán et al. (2013) at plot scale (but for water erosion). Typical macro-tracers are coloured stones (Turkelboom et al., 1997; Thapa et al., 1999; Kietzer, 2007; Tiessen et al., 2007; Zhang and Li, 2011; Logsdon, 2013) and different types of metal, mostly aluminium cubes (Lindstrom et al., 1990; Van Oost et al., 2000; Van Muysen et al., 2002; De Alba et al., 2006; Barneveld et al., 2009), which are often individually numbered. In addition, approaches that attempt to mimic soil with the intention of more realistically simulating soil movement have been used (e.g., coloured aggregates, Dupin et al., 2009). The main advantage of these macro-tracers is that in most cases the movement of individual, numbered particles can be tracked. The main disadvantage is the very time-consuming application and especially the recovery of the particles from the tilled soil layer.

The most widely used in-situ tracer to determine tillage (or total) erosion is ^{137}Cs resulting from atom bomb testing in the 1950s and 1960s (Quine et al., 1994; Govers et al., 1996; Quine et al., 1996; Van Oost et al., 2003; Heckrath et al., 2005; Kietzer, 2007). Tillage erosion rates are estimated by comparing the ^{137}Cs activities at different slope positions and soil depths with those of reference sites that should not be affected by any soil erosion or deposition. A similar approach is based on other naturally occurring tracers, e.g., Jordanova et al. (2011) used the natural magnetism in different soil horizons to determine tillage erosion and deposition due to different depths of these horizons. The advantage of using these kinds of natural tracers is that they represent long-term (decades to centuries) erosion. Apart from technical issues with these techniques, their major disadvantage is that they do not only measure tillage erosion because the pattern of tracer redistribution results from the combination of various erosion types (Van Oost et al., 2006).

Techniques to estimate tillage erosion from changes in topography vary widely regarding their spatial and temporal resolution. In several studies, the slight step in topography introduced by tillage at the upslope boundary allowed the translocation of soil material to be determined due to tillage at the upslope end of experimental plots (Turkelboom et al., 1997; Kimaro et al., 2005). This so-called step method has been combined with the installation of soil collecting trenches at the downslope end of the experimental plots (Turkelboom et al., 1997; Kimaro et al., 2005). Another method for the determination of elevation differences is the measurement of the soil depth above a known reference point buried below the tillage depth, e.g., a concrete block as in Sadowski and Sorge (2005).

Photogrammetry was used by Vandaele et al. (1996) to carry out a longer-term and larger-scale estimate of tillage erosion. They determined temporal patterns of elevation differences using sequential stereoscopic aerial photographs from the Belgium loess belt (1947–1996). Their findings underlined the importance of tillage erosion in the region, with the most severe surface lowering occurring on hilltops and on hillslope convexities (Vandaele et al., 1996). More recently, high-resolution digital elevation models (DEMs) in combination with digital aerial photographs have improved long-term analysis of landscape changes (Deumlich et al., 2014) and recent advances in image acquisition and software have, over the past decades, made novel measurement techniques for geomorphological change detection affordable. Terrestrial laser scanners (TLS) and unmanned aerial systems (UAS) together with structure from motion (SfM) techniques have been utilized in several morphological change detection studies. On arable land the majority of these studies have focused on rill and gully erosion features (d'Oleire-Oltmanns et al., 2012; TLS: Eltner and Baumgart, 2015; UAS: Peter et al., 2014; Eltner et al., 2015; Vinci et al., 2015). A recent study by Pineux et al. (2017) investigated spatial elevation changes at the catchment scale, utilizing multi-temporal DEMs of difference (DoD) using UAS-based SfM (UAS/SfM). However, as with natural tracers, the changes in topography result from a combination of erosion processes, which need to be unravelled for tillage erosion to be studied.

The results of tillage erosion studies (e.g., summarized in Van Oost et al., 2006) have been used to develop and parameterize a number of tillage erosion models of different complexity. The most widely used is a diffusion-type approach developed by Govers et al. (1994) that simulates tillage erosion as a function of local slope and a tillage transport coefficient k_{till}. The tillage transport coefficient generalizes several parameters (e.g., tillage speed, implement shape, soil physical properties) and needs to be determined experimentally (e.g., Van Muysen et al., 2000; Kosmas et al., 2001; Heckrath et al., 2006) or calculated from empirical relationships based on experiments (Van Muysen and Govers, 2002; Van Muysen et al., 2002). An overview of different k_{till} values for different soils, tillage depths, tillage directions, implements and speeds as well as plough layer bulk density is given in Van Oost et al. (2006). However, our knowledge of the changes in k_{till} for different tillage techniques is very limited (De Alba et al., 2004, 2006), and data regarding reduced tillage are especially rare (Van Oost et al., 2006). Apart from models using the diffusion-type approach (e.g., WaTEM-SEDEM or SPEROS-C: Van Oost et al., 2000; Van Rompaey et al., 2001; Fiener et al., 2015; Van Oost et al., 2005) there are other, more complex models taking a larger number of parameters into account, e.g., tillage direction, on-field objects, or complex field boundary effects (TILDA: Quine and Zhang, 2004; CATT: Vanwalleghem et al., 2010; TELEM: Vieira and Dabney, 2011).

All commonly used tillage erosion models are developed and tested against tillage erosion measurements. To represent individual tillage management practices, these models need to be parameterized using experimentally determined tillage erosion rates. As indicated above, there is still a lack in knowledge regarding model parameters, especially for the large number of different tillage implements (size, depths, shape, etc.). However, to establish a substantial database of model parameters to simulate tillage erosion, we first need more information regarding the comparability of different methods to determine tillage erosion. Experimentation is critical for determining the parameters used to drive tillage erosion models. Therefore, it is vital to understand how the experimental technique deployed influences the derivation of the model parameters and how these differences translate into uncertainty surrounding predictions of tillage erosion. Here for the first time we directly compare a range of methodologies for determining tillage

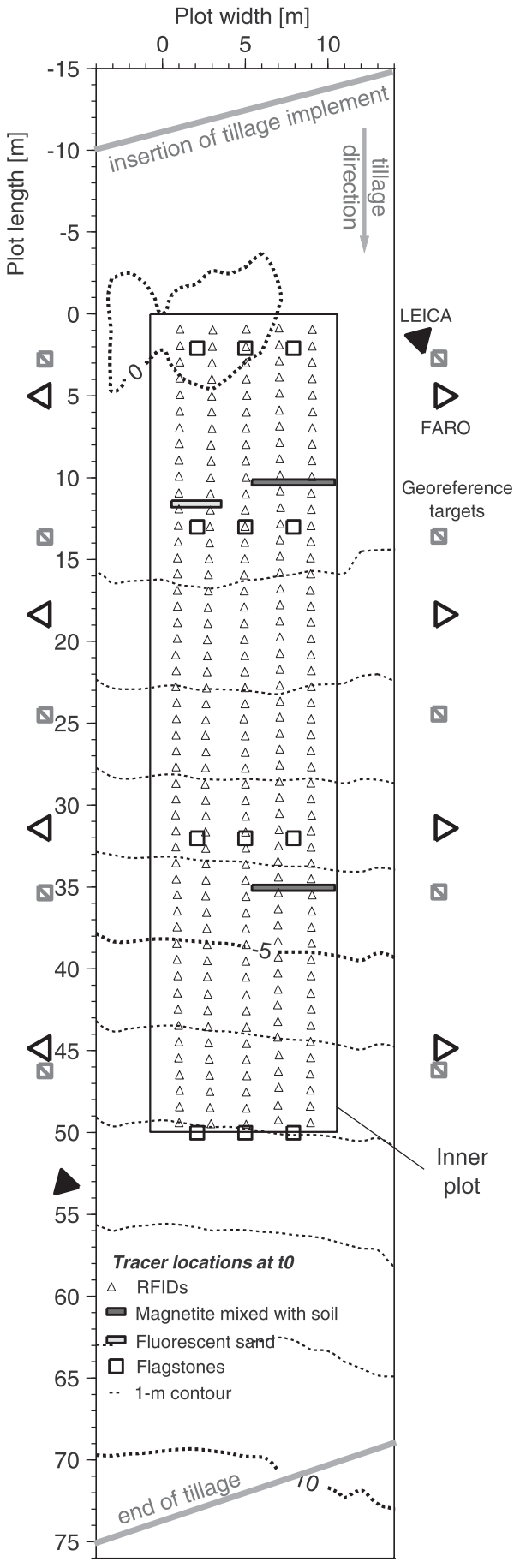

erosion simultaneously in the field. In addition, the work contributes new knowledge on the redistribution of soil in reduced tillage systems and the potential of new tracer methods and topographic change techniques to quantify tillage erosion rates.

The main aims of the study are (i) to quantify and compare tillage-induced soil redistribution using different tracers and high-resolution topography measurements, and (ii) to quantify potential differences between tillage erosion measuring techniques and discuss corresponding uncertainties for soil erosion modelling resulting from different model parameters derived from different measuring techniques.

2. Materials and methods

2.1. Test site and experimental design

The experimental site was located near the village of Polßen (53.157° North; 13.962° East) about 80 km northeast of Berlin, Germany. It represents the typical topography of previously glaciated, hummocky ground moraines. The soils in this region are strongly affected by landscape position. Extremely eroded Calcaric Regosols (IUSS, 2015) are often located at the hilltops, whereas moderately to strongly eroded Luvisols can be found along the slope, and colluvial, partly groundwater-influenced soils are located in closed depressions (Sommer et al., 2008; Gerke et al., 2010). The subcontinental climate in the area is characterized by a mean annual precipitation of approximately 500 mm a^{-1} and a mean annual air temperature of 8.9 °C (CLINO-1981–2010 for the meteorological stations Gruenow and Angermuende). The region is intensively used for agricultural production with large fields (>20 ha) cultivated using heavy farming equipment since the early 1970s (Sommer et al., 2008).

The experiment was performed between 03/04/16 and 08/04/16 on a convex upslope, located within a large (~50 ha) field where winter wheat had been planted in autumn. Overall, an area of 15 m × 85 m was prepared with an inner plot of 10 m × 50 m where the tracers were placed (Fig. 1). To homogenize the soil and bury the germinated wheat on the test field, the plot was firstly tilled (03/04/16) with a mouldboard plough to a depth of 0.25 m and then smoothed with a roller. Subsequently, the time after initial plot preparation is referred to as t0. For the (reduced) tillage erosion experiment, two sequences of seven downslope tillage operations consisting of a combination of a cultivator and a roller were applied on 04/04/16 and 06/04/16. Subsequently, the time after the first and second tillage sequence is referred to as t1 and t2, respectively. The cultivator, a Tiger 4 AS (HORSCH Maschinen GmbH; Germany), consisted of a series of disks, tines and a roller, and tilled the soil to a depth of 0.15 m without inverting but disrupting and mixing the soil. The tillage width of the cultivator was 5 m, requiring three parallel downslope operations for one cultivation of the plot. The tractor speed during tillage was approximately 6 km h^{-1}. The roller had a width of 7.5 m, hence only two passes were necessary for rolling the plot.

To monitor potential bulk density changes between t0 and t2, it was measured at 20 locations within the inner plot (centre of 5 × 5 m rasters) at two depths (0.06 to 0.12 m and 0.18 to 0.24 m, respectively) using Kopecky cylinders with a diameter of 0.08 m (volume 3.0 × 10^{-4} m^3; Table 1).

2.2. Tracer techniques

2.2.1. Micro-tracers

Magnetic iron oxide mixed with soil: A total of 312 kg of soil were mixed by serial dilutions with magnetic iron oxide (subsequently referred as magnetic tracer) to increase the average background

Fig. 1. Topography of the test site, location of tracers at the beginning of the experiment (t0), TLS scan positions, and location of georeferenced targets for TLS and UAV/SfM measurements.

Table 1
Bulk density and stone content measured after preparation of the plot with one-time ploughing to a depth of 0.25 m (t0) and at end of the experiment after 14-times tillage with the field cultivator to a depth of 0.15 cm (t2).

Parameter	Soil depth (m)	Time	Mean	Standard Dev.	Min	Max	n
Bulk density incl. stones ($t\ m^{-3}$)	0.06–0.12	t0	1.53	0.08	1.36	1.70	20
	0.18–0.24	t0	1.56	0.11	1.40	1.78	20
	0.06–0.12	t2	1.60	0.08	1.48	1.79	19
	0.18–0.24	t2	1.67	0.13	1.47	1.88	20
Stone content (mass-%)	0.06–0.12	t0	14	4.3	9	25	20
	0.18–0.24	t0	13	3.9	7	22	20

concentration of soil by two orders of magnitude following the protocol of Guzmán et al. (2010). Magnetic iron oxide mainly binds to the fine particle fraction (clay and silt) of the soil. The mixture was applied at t0 in two trenches of 5.0 m × 0.35 m × 0.15 m (width perpendicular to slope, length along the slope, depth) on the upper and middle right side of the plot (Fig. 1). Volumetric magnetic susceptibility at the beginning of the trial and after every tillage sequence (t1 and t2) was measured using a MS2 sensor and a MS2D field probe (Bartington Instruments, UK). The device penetrates the soil and integrates the signal with depth (10% of the signal is associated to a depth of response of 0.06 m). A 0.90 m × 2.50 m grid (X, Y) was set out, with a more dense measuring grid (Y distance: 1.25 m) at areas close to the initial tagged trenches. In order to calibrate the signal of the field probe and allow conversion of the volumetric magnetic susceptibility into the mass of tracer, a total of 18 random locations (including originally untagged areas and trenches) were sampled before and after the first seven tillage passes at different depths (0–0.05 m, 0.05–0.10 m, and 0.10–0.15 m). Their magnetic susceptibility was determined using a MS2B laboratory meter (Bartington®) as described by Guzmán et al. (2013, 2015). Additionally, samples below the tillage layer (interval 0.15–0.20 m) were taken and analysed in the laboratory to evaluate and calibrate the field probe.

Fluorescent sand: The fluorescent tracer is commercially-available (Partrac Ltd.; UK) and consists of natural quartz particles (D_{50} = 70 μm) coated with a green fluorescent pigment. A Panasonic Lumix GH4 camera was used with an orange 490 nm long pass filter (Knight Optical; UK) to enhance the contrast between the soil and the tracer. Images were taken during the night or under darkened conditions using an external LED light source (wavelength = 450 nm) with diffusing plates to produce the fluorescent response. An intensity-based method, similar to that of Hardy et al. (2016) was utilized to analyse the amount of tracer in the images. The intensity-based method used the numeric pixel values from the green colour channel in the camera and differentiates between the background intensity of the soil and the fluorescent tracer. Therefore, a reduction of the tracer concentration and corresponding soil flux can be derived. At t1 a trench (3.0 × 0.4 × 0.15 m; Fig. 1) was filled with the fluorescent tracer particles and the intensity-based method used to determine the tracer redistribution was used at t2. Therefore, the visible surface intensity was determined and the depth distribution of the tracer was measured in five 1.0 m × 0.2 m × 0.15 m trenches downslope from the tracer application trench (distance: 2.5, 5.0, 7.5, 10.0, and 12.5 m).

2.2.2. Macro-tracer

Passive radio-frequency identification transponder: Commercially-available passive radio frequency identification (RFID; HID Global, Germany) transponders were used together with a newly designed prototype detection antenna (diameter 0.2 m; TECTUS Transponder Technology, Germany) to tag soil movement along the inner plot. RIFD transponders (n = 250), grouted in glass cylinders (4 mm × 22 mm; density = 2.3–2.5 $g\ cm^{-3}$), were inserted to a soil depth of 0.075 m (mid tillage depth) along five rows (spacing of rows and along slope 2 and 1 m, respectively; Fig. 1). At t1 and t2 the RIFD transponders were re-located with the detection antenna, and the new location of the transponders was determined with a total station (TS 06 plus R1000; Leica, Germany). Individual horizontal displacement distances of the RFID transponders were calculated, both along and perpendicular to the slope and tillage direction.

2.3. Topographical techniques

2.3.1. Flagstones

Concrete flagstones (n = 12; 0.25 m × 0.25 m × 0.03 m) were buried at t0 at different slope positions to a mean depth of 0.42 m (Fig. 1). To relocate the flagstones after the tillage sequences, 3 M™ Full-Range Markers (3M™, US; 0.38 m diameter) were buried underneath the flagstones. The markers allow for a precise relocation of the flagstones after the tillage sequences by using a 3 M™ Dynatel™ Locator (detection range of about 2.5 m). The change in soil depths above the flagstones at the tillage sequences t1 and t2 were measured with a 0.8 m long soil probe (steel needle). Measurements at t1 and t2 were corrected for changes in bulk density and hence surface elevation (see below).

2.3.2. Terrestrial laser scanning

Two different impulse wave terrestrial laser scanners (TLSs), a Leica (Scanstation C10; Leica, Germany) and a Faro (Focus 3D; FARO, US), were used during the experiment. The Leica TLS has a lower spatial resolution with a scanning range of ~300 m, while the Faro TLS has a higher spatial resolution with a maximum scanning range of ~50 m. The Leica scans were performed from two locations at the upper and lower end of the plot, while the Faro scans were taken from eight locations (four on each side of the plot; Fig. 1). An average resolution depending on the distance between scanner and soil surface of 4.4 × 10^3 and 175 × 10^3 points per m^2 was achieved for the Leica and Faro scanner, respectively. Each scan took about 60 min with the Leica and about 12 min per scan with the Faro.

To georeference the scans, ten static black and white targets were equally distributed along plot borders (Fig. 1) and independently located for each time step (t0–t2) with a total station (TS 06 plus R1000; Leica, Germany). The reference coordinates were used to register the TLS data into a single merged point cloud for t0, t1, and t2 using the Leica software Cyclone 9 (Leica, Germany). Digital elevation models of different grid size resolutions of the merged point clouds were processed in CloudCompare 2.6.2 (cloudcompare.org). Subsequently, DoDs were calculated using R for statistical computing 3.2.2 (R Development Core Team, Austria) and ArcGIS 10.4.1 (ESRI, US).

2.3.3. UAS/SfM

DEMs for the time steps t0 and t2 were calculated using the UAS/SfM technique. Therefore, a hybrid Sony α5000 camera with a 20.1 MP (5456 × 3064 pixel) resolution was mounted on a gyro-stabilised gimbal to a multirotor UAS platform. The UAS was a custom built hexacopter with a double rotor setup on three arms (RcTakeOff, Belgium). The images (t0: n = 99 images; t2: n = 88 images) were recorded from a nadir angle with a 16 mm focal length, f 3.5–5.6 OSS (equivalent 24 mm) and an average flight elevation of 15 m. The TLS black and white targets were also used for referencing the SfM approach. SfM calculations were carried out using PhotoScan Professional version 1.0.4 (Agisoft; Russia) and for further point cloud processing, the software CloudCompare 2.6.2 (cloudcompare.org) was used. The average point cloud density of the inner plot is 75 × 10^3 points per m^2.

2.3.4. Determining change in topography

To calculate spatially distributed erosion and deposition from the different TLSs and UAS/SfM based DEMs at t0, t1 and t2, it was necessary to correct these DEMs for bulk density changes during the experiment. Therefore, the measured changes in bulk density (t0 and t2; Table 1) were used to correct for the settling of the soil surface during the experiment. It was assumed that the increase in bulk density happened solely

in the tillage layer between t0 and t1 as complete disruption was reached after seven tillage operations and soil loosened during the pre-experimental mouldboard ploughing to a depth of 0.25 m had settled. To validate this assumption, the mean elevation change over the entire area affected by tillage was detected using the LEICA TLS data. Between t0 to t1 the measured mean elevation difference was −20 mm, while between t1 and t2 the measured mean elevation difference was negligible (< 0.1 mm), indicating no change in bulk density after t1. With this analysis in mind, we used the measured mean bulk density change from the 20 locations (Table 1) between t0 and t2 to correct for the higher mean elevation of the plot at time t0, which resulted from lower bulk density after mouldboard ploughing. Overall, the initial DEM (t0) was lowered by −13.2 mm.

2.4. Calculating downslope soil flux from tracer movement and topography changes

To derive soil translocation distances and translocation rates from the different measuring techniques, two approaches were applied. First, the soil translocation distance was derived directly from the measured translocation distance of the respective tracer. The underlying assumptions here are that the translocation distance of the tracer represents the translocation distance of the tilled soil layer, the transport distances of the tracer are normally distributed (and hence, the mean transport distance adequately represents its movement), and the tracers are more or less homogenously moved throughout the depth profile of the tillage layer. The distribution of the tracer movement was tested with all tracers and any depth dependence was tested according to depth profiles of the fluorescent tracer along the slope and point measurements of the magnetic tracer. For the RFIDs a mean or median translocation distance in the inner plot was calculated from the movement of all recovered individual RFIDs; non-recovered RFIDs were assumed to travel the mean distance determined from those that were recovered. Due to the large number of RFIDs distributed over the inner plot (Fig. 1), it was also possible to calculate movement parallel and perpendicular to the slope. Moreover, movement at different slope positions could be determined between t0 and t1 as well as t1 and t2. In the case of the micro-tracers, the mean or median translocation distance was derived from the distribution of the measured tracer intensity (magnetic susceptibility and fluorescence) downslope the application trenches. It is important to note that in the case of magnetic susceptibility the bulk magnetic susceptibility of the plough layer is measured, while in case of fluorescence only the distribution of particles on the soil surface was determined. Compared to the RFIDs, it was only possible to determine tracer movements from one (fluorescent tracer) and two locations (magnetic tracer) and one time step. Based on the translocation distance, a mean soil translocation rate was calculated following Eq. (1), while using the measured mean bulk density (Table 1) and a mean tillage depths of 0.15 m (Van Oost et al., 2006):

$$Q_s = \rho_b \cdot \bar{d} \cdot D \tag{1}$$

where Q_s is the rate of soil translocation (kg m^{-1}); ρ_b is the soil bulk density (kg m^{-3}); $\bar{d}$ is the tillage translocation distance (m), and D is the tillage depth (m).

Second, based on 0.5 m × 0.5 m raster DEMs determined from the three different topographical techniques, the average translocation distance and soil translocation rate was calculated. The tillage translocation started at the upslope end of the plot where the plough was inserted to the soil (plot length location of about −12.5 m; Fig. 1). The calculation follows the conservation of mass and routes the soil movement (the slope is subdivided into 1 m segments) from the source area down to the lowest increment. Hence, even without a change in topography (in-flux equals out-flux), e.g., at a mid-slope location, the soil translocation rate and distance can be derived using Eqs. (1) and (2). The tillage translocation distance ($\bar{d}$; m) at each 1 m segment i was calculated as:

$$\bar{d}_i = \frac{V_i}{W \cdot D} \tag{2}$$

where V is the volume of soil loss (m^3) from the tillage implement insertion to segment i, D is the tillage depth (m), and W is the plot segment width (m).

3. Results

3.1. Translocation of tracers

All the tracers showed a substantial downslope movement after 7 and 14 tillage passes (Fig. 2), with a maximum movement of up to 18 m recorded for an individual RFID during one of the tillage sequences. Across all the tracers, mean translocation distances per tillage pass had a substantial range of 0.23 m to 0.71 m that depended on the tracer and slope position. Deriving a probability density function of the mean tracer movement per tillage pass of all RFIDs between t0 and t1 (recovery rate 79%) as well as t1 and t2 (recovery rate 75%) indicates that a forward movement of RFIDs only occurred parallel to the slope, while perpendicular to the slope the mean movement was close to zero (Fig. 3). Hence, we subsequently only analysed the movement of tracers in the downslope direction.

Comparing the movement of the RFIDs located around the micro-tracer trenches (maximum distance upslope and downslope of application trench ≤5 m) with the movement of the magnetic tracer (two trenches (Fig. 1); t0 to t1) and fluorescence tracer (one trench (Fig. 1); t1 to t2) indicates a substantial difference in movement between the micro-tracers and the macro-tracer (Fig. 4; Table 2). In all cases the micro-tracers exhibited a larger translocation distance, while their behaviour at different slope positons was consistent, e.g., at the upper and lower trench of the magnetic tracer (Fig. 4A vs. Fig. 4B). Larger transport distances were measured for all tracers on steeper slopes. The mean translocation distance per tillage pass was 26 ± 12% less for the RFIDs compared to the micro-tracers (Table 2).

Measurements of the fluorescent tracer in five soil pits (0–0.15 m) downslope of the tracer application trench at distances of 2.5, 5.0, 7.5, 10.0 and 12.5 m indicate some soil disturbance along the soil profile (Fig. 5, Table 3) without an obvious systematic depth dependency. Hence, the surface luminescence corresponds to the total movement of the tillage layer. The surface measurements of the fluorescent tracer indicate that after seven tillage passes only 17% of the tracer was still located in the area above the first soil pit (2.5 m below application trench). Hence, it was assumed that the depth measurements represent 83% of all fluorescent material to be detected, while ignoring potentially small tracer amounts moved >15 m below the application trench. Under this assumption the relative amount of the fluorescent tracer and its mean translocation distance in each of the 0.01 m soil layers could be calculated (Table 3). According to this calculation, no systematic depth dependency in amount and translocation distance ranging from 0.68 to 0.83 m per tillage pass (mean ± sd = 0.76 ± 0.05 m) could be detected. This finding was corroborated through six magnetic tracer measurements at three depths (0–0.05 m, 0.05–0.10 m, 0.10–0.15 m) downslope of the tracer application trenches (1.25 m, 2.5 m, 3.75 m, 5.0 m) that only showed slightly higher, but insignificant ($p < 0.05$) values for the soil movement in the upper topsoil layer (0–0.05 m). Both the fluorescent and the magnetic tracer indicate that the different transport distances of the tracers cannot be explained from the different application depths of 0–0.15 m in the case of the micro-tracers and 0.075 m in the case of the RFIDs.

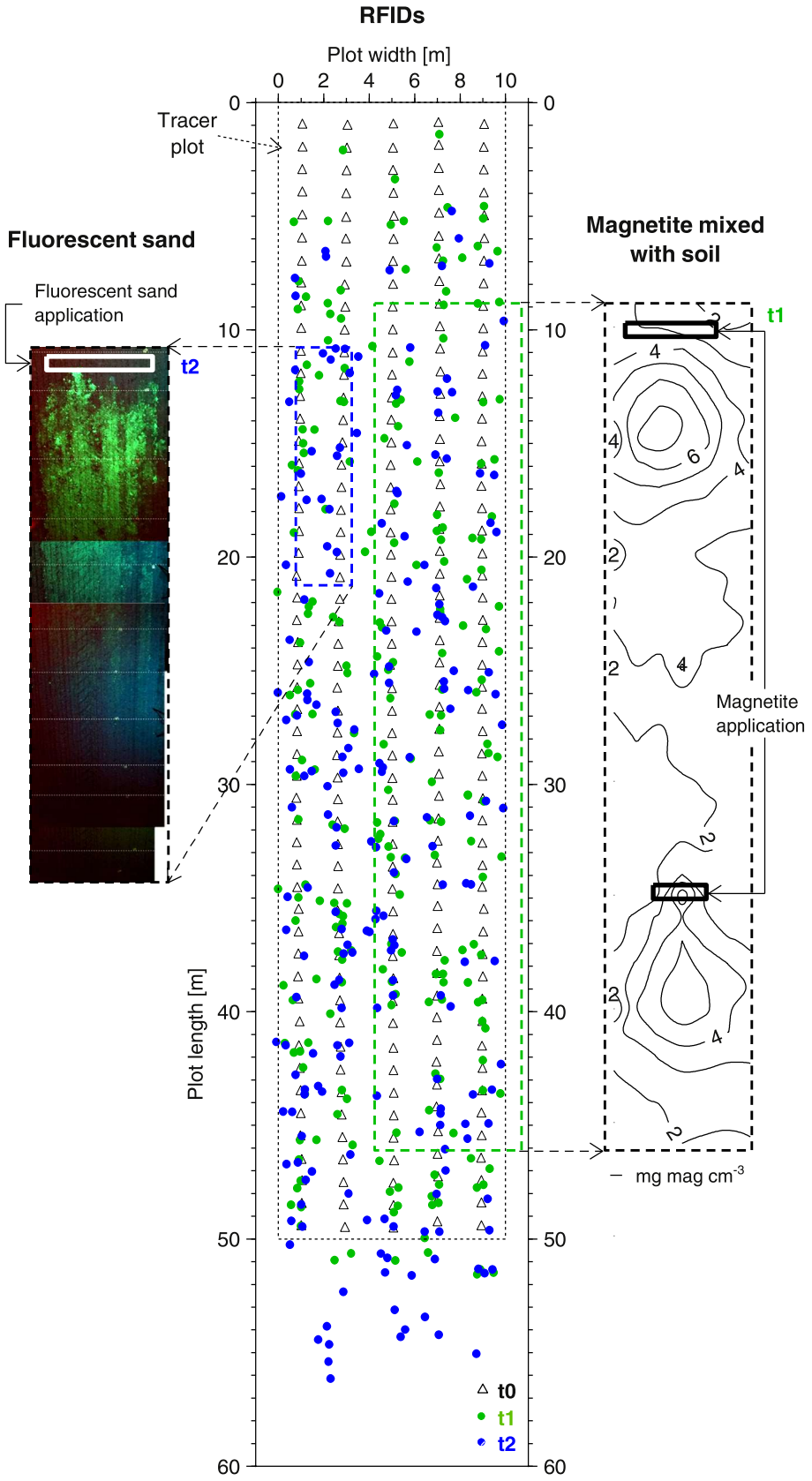

Fig. 2. Translocation of individual RFIDs (t0 to t1 and t1 to t2); translocation of magnetic tracer mixed with soil from trenches 1 and 2 (t0 to t1) given as lines of equal magnetisation (mg mag m^{-3}); translocation of fluorescent sand from trench 3 (t1 to t2) given as mosaic of colour images taken under an external light-source.

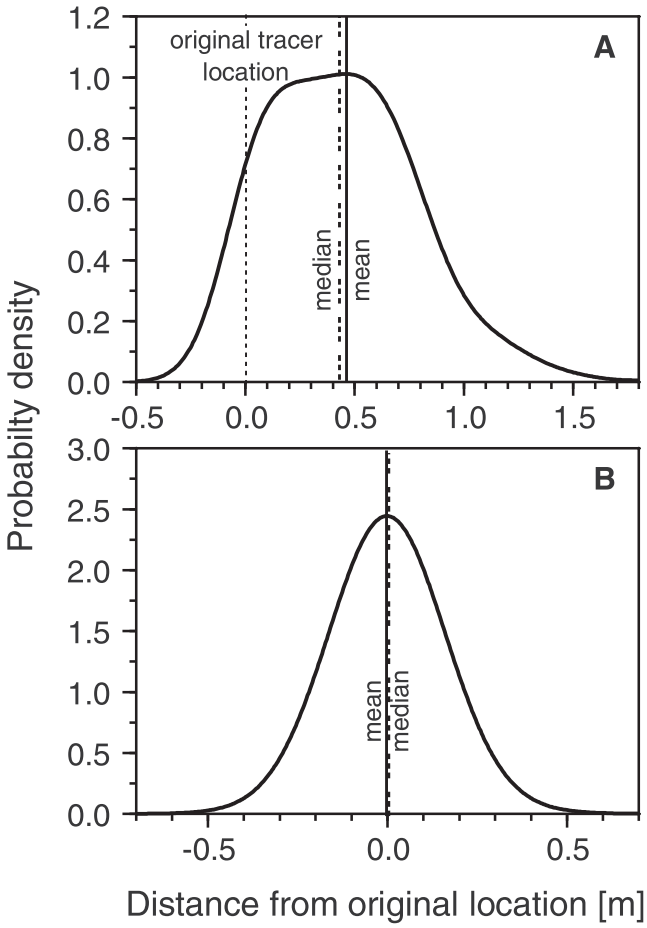

Fig. 3. Mean and median translocation of all RIFDs per tillage pass (t0–t1 and t1–t2); in slope direction (A) and perpendicular to slope direction (B).

3.2. Change in topography

The DoDs between the start and the end of the experiment (t0–t2) show good agreement in spatially distributed erosion and deposition patterns for all measuring techniques (Fig. 6). The absolute elevation differences between the TLS systems at the time t0 to t1 accurately match for both the flagstone positions and the gridded DEM data (Table 4). The TLS systems indicate a substantially lower loss for the tillage sequence t1 to t2 compared to t0 to t1. However, for tillage sequence t1 to t2 the Leica shows a lower soil loss than the Faro. In contrast to the TLS systems, the UAV/SfM show a net soil gain within the inner plot between t0 and t2 (Table 4). The flagstone point measurements for t0 to t2 are in the same range as the TLS measurements, but show major deviations compared to the TLS systems for the individual tillage sequences (Table 4).

3.3. Soil translocation distances and translocation rates

Based on Eq. (1), the depth-independence of tracer movement (Table 3) and the close to normal distribution of tracer movement (Figs. 3 and 4), we calculated the mean soil translocation distance and rate per tillage pass for each original tracer location. For the florescent and the magnetic tracers soil translation was determined for the upper and lower trench locations at the tillage sequence t0–t1 and t1–t2, respectively (Fig. 7). For the RFIDs, soil translocation was calculated for ten 5 m segments of the inner plot (Fig. 1) for both tillage sequences. Compared to the single trenches or segments along the slope soil translocation was derived in 1 m segments from the DoDs of the TSL systems

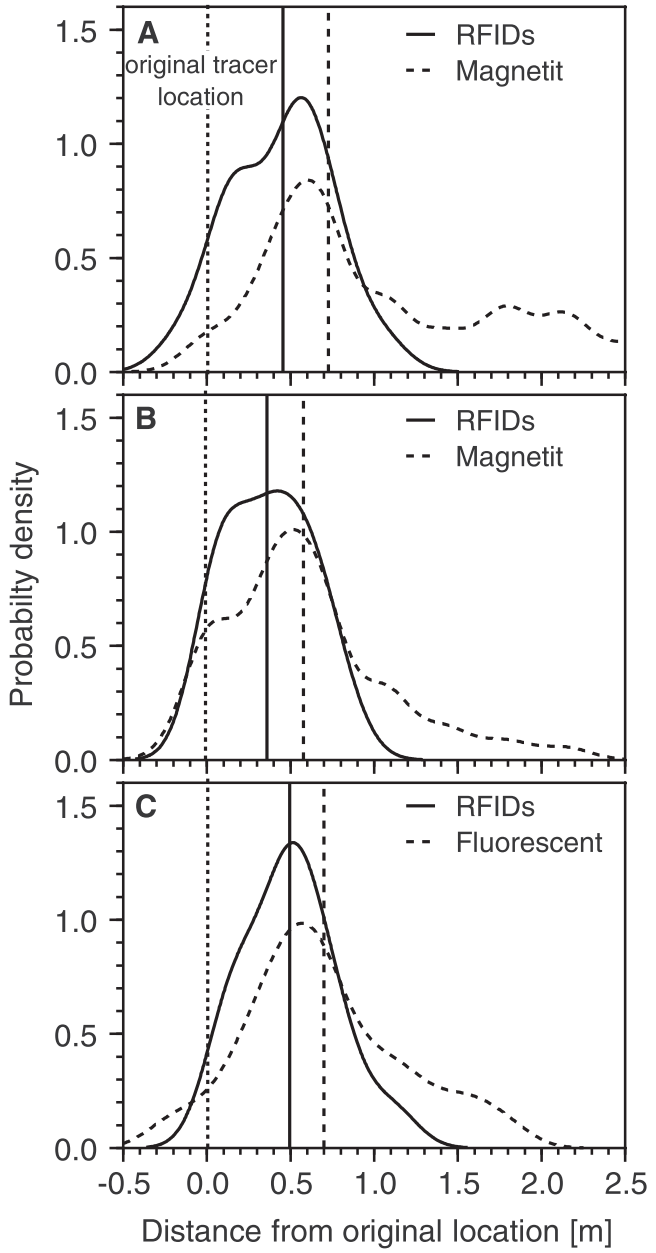

Fig. 4. Comparison of mean translocation distance per tillage pass of different tracers. RFIDs vs. magnetic tracer translocation from upper (A) and lower trench (B) between t0 and t1. RIFDs vs. fluorescent tracer translocation from upper trench between t1 and t2; It is important to note that in case of the RFIDs slope segments (max. distance upslope and downslope of micro-tracer application trenches ≤5 m) are compared against tracers distributed along small trenches (see Fig. 1). The solid and dashed vertical line shows the average transport distance of the RFIDs and the corresponding micro-tracer, respectively.

Table 2
Mean tracer translocation at magnetic tracer trenches and at fluorescent trench according to probability density functions.

Tracer	Tracer origin	Time of measurement	Mean translocation per tillage (m)
Magnetic tracer	Upper trench	t1	0.71
RFIDs			0.44
Magnetic tracer	Lower trench	t1	0.59
RFIDs			0.37
Fluorescent tracer	Upper trench	t2	0.70
RFIDs			0.50

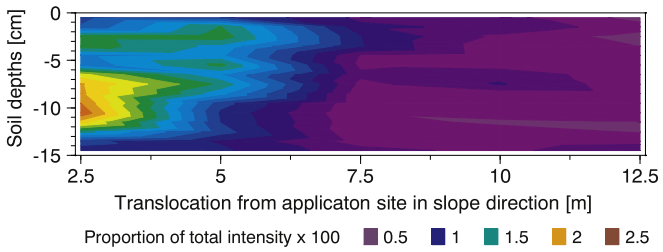

Fig. 5. Soil depths-dependent translocation distance of fluorescent sand during seven tillage passes; translocation from upper trench between t1 and t2.

using Eq. (1) and Eq. (2). Soil translocation was not calculated for the UAS/SfM system, as the point of implement insertion was unfortunately not recorded.

The soil translocation distances and rates from the different techniques showed some consistencies but also some substantial differences (Fig. 7). The Faro and the micro-tracer distances and rates were very similar and additionally the Faro translocation did not substantially change between t0–t1 and t1–t2. In contrast, the Leica translocation showed some substantial difference between t0–t1 and t1–2, with a difference in mean translocation rates of 80.6 kg m^{-1} per pass (difference of t1–t2 relative to t0–t1 is 47%). As expected from the tracer flux calculations, the RFID-based soil translocation distances and rates were substantially smaller than those of the micro-tracers, and were closest to the Leica derived data for the tillage sequence between t1 and t2. Comparing all data (both tillage sequences) for the areas around the tracer trenches (between 7.5 m and 17.5 m and 32.5 m and 42.5 m) indicates, that the different techniques resulted in a substantial variability of derived soil translocation rates ranging from 105.6 to 170.4 kg m^{-1} per pass at the upper trench area and from 80.9 to 175.6 kg m^{-1} per pass for the lower trench area. Even more extreme differences can be recognized for the downslope end of the inner plot where four-fold differences between RFID-based and Leica-based translocation rates were found (t0–t1; Fig. 7).

4. Discussion

4.1. Implications of measurement uncertainties

A number of studies were performed over the last two decades reporting different soil translocation rates for different soils (properties, conditions) and tillage techniques (tillage speed, direction, depth, type of implement, etc.) determined from a variety of measurement techniques (e.g., Van Muysen et al., 2002; Van Oost and Govers, 2006; Kietzer, 2007; Tiessen et al., 2007; Barneveld et al., 2009; Logsdon, 2013). Van Oost et al. (2006) provide a comprehensive overview of results acquired until 2006. From these data it is obvious that there are substantial differences for similar tillage categories (e.g., mouldboard tillage), which were mostly interpreted as differences resulting from differences in soil properties (bulk density) and in tillage technique (especially tillage depths, tillage speed, and tillage direction; Lobb et al., 2001; Van Oost et al., 2006). However, uncertainties associated to different measuring techniques used in different studies were not systematically analysed.

Assuming that the results of the individual techniques presented in this study, which were carried out under optimal conditions and the use of high precision equipment, are of comparable quality to those referred to by Van Oost et al. (2006), our work indicates that substantial uncertainties in estimated tillage erosion rates not only result from different experimental set-ups but also from the different techniques used. For those areas of the tested slope where the different techniques can be directly compared we could identify substantial differences in soil translocation rates per tillage pass (upper trench: 106–170 kg m^{-1} per pass, difference = 60%; lower trench: 81–176 kg m^{-1} per pass, difference = 118%; Fig. 7). Comparing the mean translocation rate from six measuring techniques that represent three basic types of tillage erosion determination (micro-tracer, macro-tracer, topography) and two tillage sequences against the corresponding individual measurements, ranges from an underestimation of −32.8 kg m^{-1} (−21.6%) to an overestimation of 41.3 kg m^{-1} (33.6%). When using experimental results to parametrize tillage erosion models (Van Oost et al., 2005; Dlugoß et al., 2012), these measurement uncertainties need to be added to uncertainties based on the transfer of measured tillage erosion rates from one test site to another modelling region. The relevance of this uncertainty was recently illustrated by Wilken et al. (2017), who coupled a water and tillage erosion model and a soil organic carbon model to analyse erosion-induced carbon (C) fluxes in a small catchment. Varying tillage erosion by ± 50% substantially changed the modelled erosion-induced C balance of the catchment, which was overall more important for the C balance than water erosion (Wilken et al., 2017). In general, it can be concluded that tillage erosion measurement uncertainties of the magnitude found in this study can substantially affect the results of studies dealing with erosion-induced changes in soil properties of arable land.

4.2. Specific uncertainties of different tillage erosion measuring techniques

Micro-tracer methods disturb the natural soil structure because a trench is filled with artificial or artificially manipulated soil material. This causes uncertainties regarding the transport and mixing properties of the tracer particles into the natural soil structure. If applied in a trench, the fluorescent tracer concentration can reach the detectable saturation level. As a consequence, the peak concentration might not be accurately determined and causes uncertainties in the translocation calculation, which is based on fluorescence intensity proportions. RFID macro-tracers enable fast tracking of individual particles at distinct slope positions without soil disturbance (e.g., soil sieving as applied to traditional macro-tracers). The experiment showed 26 ± 12% lower translocation distances determined by the stone-sized RFID macro-tracers compared to soil-sized micro-tracers (Table 2). This calls the widely used assumption that tillage erosion is a non-selective process into question. A few studies already speculated about different transport distances between soil and stone sized tracers (Barneveld et al., 2009; Dupin et al., 2009; Logsdon, 2013), but did not investigate this in detail. Nevertheless, it is likely that a potential grain size selectivity of tillage erosion is affected by soil conditions and tillage implement type. Soil cohesiveness may control whether the soil is disrupted and

Table 3
Mean soil translocation distance per tillage pass in different 1-cm soil layers and relative translocation amount in each of the 1-cm soil layer.

Soil depths (cm)	Translocation distance (m)	Relative amount transported per layer (%)
Surface	0.69	
0…1	0.71	5.90
1…2	0.81	6.81
2…3	0.81	7.29
3…4	0.79	7.06
4…5	0.76	6.48
5…6	0.77	6.64
6…7	0.80	7.19
7…8	0.83	7.61
8…9	0.78	7.20
9…10	0.74	6.90
10…11	0.74	6.91
11…12	0.71	6.55
12…13	0.70	6.13
13…14	0.68	5.52
14…15	0.74	5.82
0…15	0.76	100

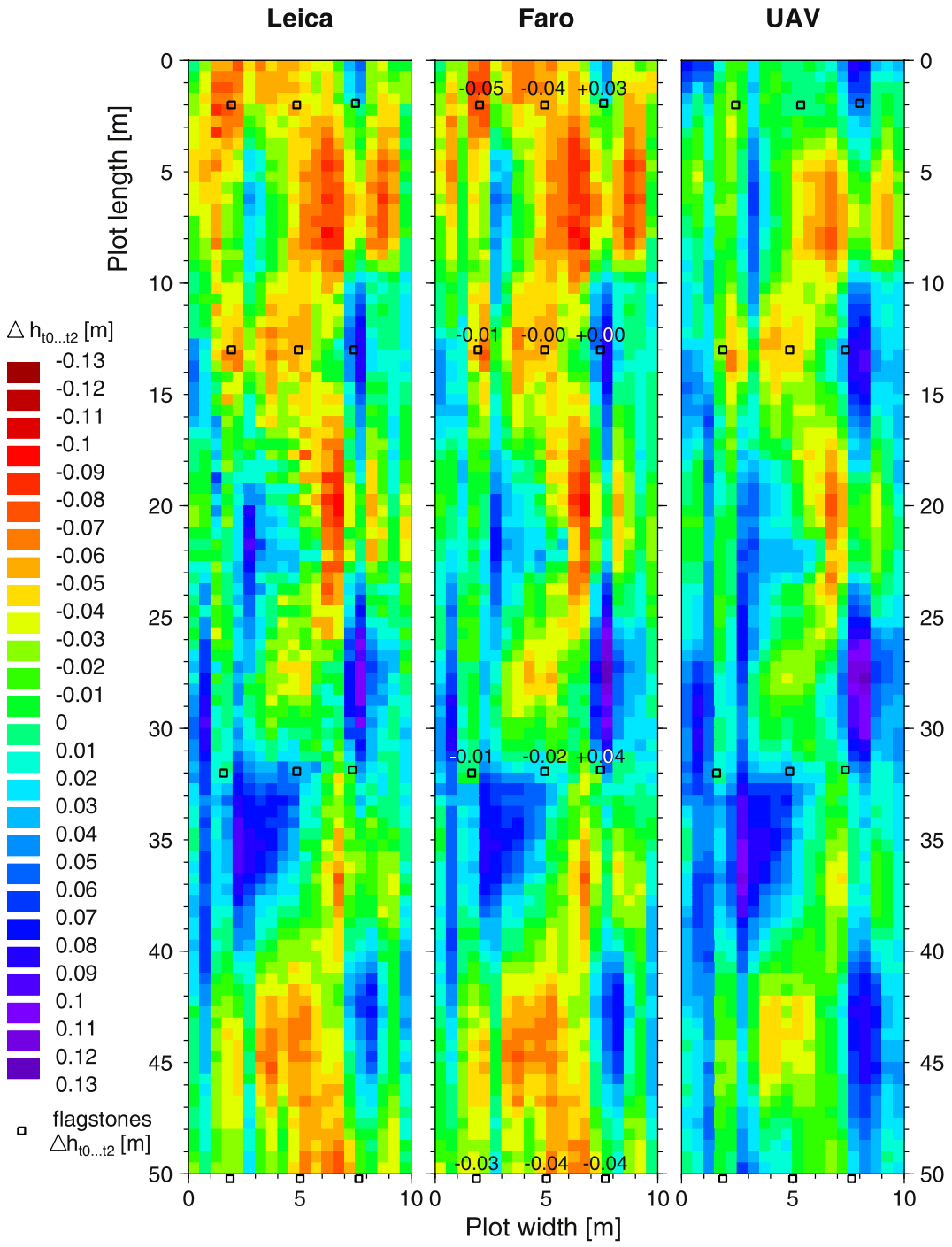

Fig. 6. Difference in topography between t2 and t0 for all measuring systems. High-resolution data degraded to 0.5 m × 0.5 m. Elevation differences derived from the flagstone technique are given in the mid (Faro) DoD map.

selectively mixed or homogenously transported in large clods that encapsulate stone-sized particles. Due to a series of tillage operations under rather dry conditions, the soil was highly disrupted during the experiment, which might have supported selectivity compared to a single tillage operation and hence the 14 applied tillage operations are not identical to 14 yr of cultivation. Furthermore, a potential grain size selectivity of tillage translocation is likely to be tillage implement specific as some implements are designed to invert topsoil and not to disrupt and entirely mix it.

High-resolution measurements of topography change can identify spatial movement of the tillage layer and are not affected by potential grain size selective transport. However, the technique needs to be corrected for elevation changes related to bulk density differences that are subject to spatial variations (Gifford and Roderick, 2003). Because TLS and UAS/SfM devices are based on optical techniques, information gaps occur behind objects that produce shaded areas. Due to soil surface roughness, the shaded areas become larger with increasing distance to the scan device as the incidence angle of the laser beam becomes smaller (Fig. 8). Because of the linear interpolation of shaded areas, the TLS scanners systematically overestimate the elevation of remote scan positions. As illustrated in Fig. 8, this effect increases with increasing surface roughness. Owing to the smooth rolled soil surface (about 2.5 cm roughness height), the wheel tracks were the most problematic element in this study. This is especially true as the depths of the wheel

Table 4
Comparison of changes in topography at the flagstone positons and for the TLS system and the UAS for the entire inner plot.

	Δh t1–t0 (cm)		Δh t2–t1 (cm)		Δh t2–t0 (cm)		
	Mean	SD	Mean	SD	Mean	SD	n
At flagstone positions							
Flagstones	−2.4	3.3	1.1	2.7	−1.3	3.0	12
Leica	−0.8	2.4	−0.4	3.1	−1.1	4.7	
Faro	−0.9	2.6	−1.0	3.4	−1.9	5.0	
UAV					0.4	3.9	
0.5 × 0.5 Raster inner plot							
Leica	−0.8	3.0	−0.1	2.8	−0.8	3.7	2000
Faro	−0.6	2.9	−0.3	2.8	−0.9	3.8	
UAV					1.1	3.4	

tracks were deeper at t0 because of a very loose soil following the pre-experimental mouldboard ploughing and rolling. The consequence was that the long range scans with the Leica, from two positions only (Fig. 1), could only partly scan into the wheel tracks, and therefore potentially underestimates deposition in these wheel tracks between t0 and t1, and hence overestimates erosion rates. In general, an image acquisition from nadir that prevents flat incidence angles is a major advantage of the UAS/SfM technique (Fig. 8).

To unify different TLS scenes or photogrammetric images, georeferenced ground control points (GCPs) are required. On arable land, plane surfaces or clear structures are not present and scene overlay depends on GCPs. As TLS devices operate from a static position on ground, fewer GCPs are required compared to the moving UAV/SfM. Hence, a dense network of GCPs is of key importance for an UAV/SfM approach on arable land to measure tillage erosion. In this experiment the UAS/SfM approach lead to similar patters but showed an elevation offset compared to the TLS measurements. This somewhat unsatisfactory result might be improved using more GCPs or by adding stable linear features along the measuring plot, which improved SfM processing. However, it was challenging to detect small (<1 cm) changes in topography if these changes had not resulted from changes in linear features (e.g., erosion rills), which makes change detection easier. Similar problems in detecting changes on non-linear soil erosion features were shown in the UAS/SfM study of Pineux et al. (2017).

Based on our experiment it was not possible to determine one measuring technique as benchmark because all applied techniques are subject to different technique-specific error sources. However, it is clear that using only one technique to determine tillage erosion, as done in the majority of studies, will lead to large uncertainties in calculated tillage erosion rates.

Apart from technical issues of determining tillage erosion, our experiment underlines the importance of tillage erosion as a driver of geomorphological dynamics. It needs to be emphasized that the applied tillage speed of 6 km h^{-1} and depth of 15 cm was substantially lower compared to the typical regional management practice with a tillage

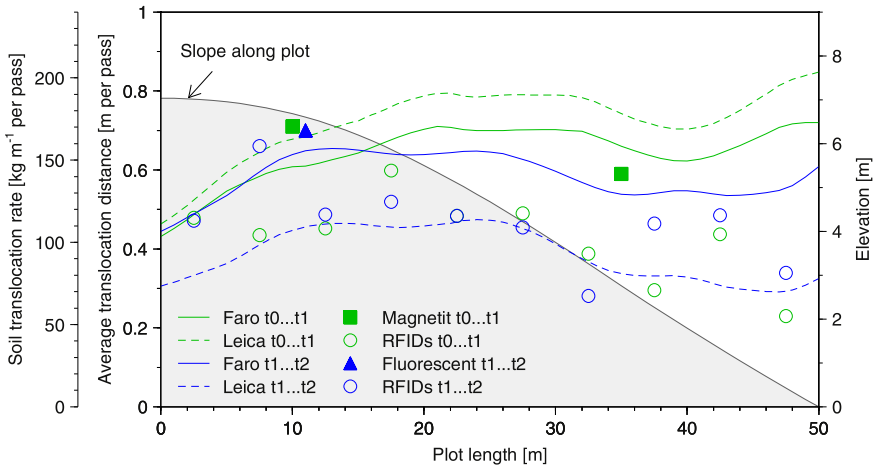

Fig. 7. Average soil translocation distance and rate derived from the different methods used between t0 and t1 and t1 and t2; movement of tracers it is indicated at the location where the tracers were originally applied; it is important to note that the movement of RFIDs is calculated in 5 m segments averages the mean movement of 4 to 31 RFIDs (mean n per segment = 20.8).

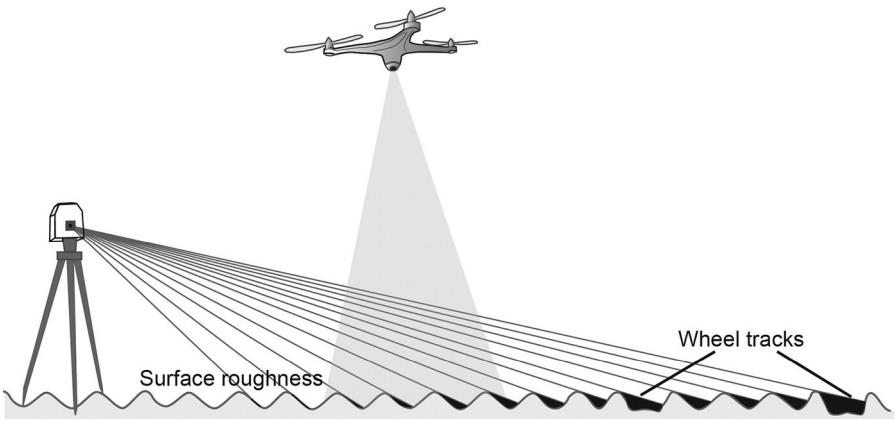

Fig. 8. Schematic figure of scan angle and shadowing effect of the laser scanners compared to UAV/SfM.

speed of 15 km h^{-1} and depth of 20 cm. Nevertheless, after 14 applied tillage operations, substantial morphological differences of approximately ± 10 cm (Fig. 6) were determined. Tillage erosion successively levels out the landscape morphology as convex hilltops are lowered and concave depressions are filled (Sommer et al., 2008). Therefore, tillage transports soil from convex areas with almost no water erosion (e.g., hilltops) to concave areas of concentrated flow and highest water erosion (Van Oost et al., 2006). Hence, on the one hand tillage removes features produced by water erosion like ephemeral gullies, but on the other hand actively supports sediment delivery by water erosion. In hummocky regions, long-term tillage erosion has an important impact on catchment topography, hydrology and soil properties.

5. Conclusion

Under controlled conditions, different tillage translocation measuring techniques (three tracers and three topographical methods) were applied in a macro-plot experiment with two tillage sequences each consisting of seven tillage operations. The different techniques produce a relatively wide range of soil translocation rates for the same slope positions, with deviations from the mean of all measurements between −32.8 kg m^{-1} (−21.6%) and 41.3 kg m^{-1} (33.6%). This large measurement-induced variation indicates substantial uncertainties in determining tillage erosion, which points to the need to utilise more than one method in tillage erosion studies. This associated uncertainty should be taken into account especially when using the results of tillage erosion experiments to parameterize models.

No benchmark result could be obtained because all of the techniques used have potential sources of error that could not be individually quantified. However, the consistently smaller translocation distances associated with the macro-tracers used, which were on average 26 ± 12% smaller than the translocation distance of the two micro-tracers, questions the widely held assumption of non-selective transport and homogenous movement of the tillage layer by management operations. At least under dry and disrupted soil conditions, as tested in this experiment, macro-tracers may not accurately represent the flux of soil-sized particles.

Compared to water erosion, we still lack standardized measurements and the overall number of measurements for different management practices is relatively small, which makes a reasonable model parametrisation challenging. Overall, this study emphasizes that tillage erosion measurements, carried out under almost optimal conditions, are subject to major uncertainties that need to be carefully considered in soil erosion studies.

Acknowledgments

The study was logistically supported by Institute of Soil Landscape Research at the Leibniz-Centre for Agricultural Landscape Research ZALF e.V. in Müncheberg, Germany. The study was supported by the Terrestrial Environmental Observatory TERENO-Northeast of the Helmholtz Association. The Fluorescent tracer work was funded by a joint U.K. Natural Environment Research Council – Analytical Chemistry Trust Fund studentship (Ne/J017795/1). Special thanks goes to Gernot Verch and Norbert Wypler. Moreover, we want to acknowledge the land owner Dietrich von Wedel allowing us to perform the experiment on his field and gave us insights regarding the regular on-site farming operations. Last but not least we gratefully acknowledge Karl Schneider from University Cologne, who initiated and financed the prototype development of the RFID antenna.

References

Barneveld, R., Bruggeman, A., Sterk, G., Turkelboom, F., 2009. Comparison of two methods for quantification of tillage erosion rates in olive orchards of north-west Syria. Soil Tillage Res. 103 (1), 105–112.

Battin, T.J., Luyssaert, S., Kaplan, L.A., Aufdenkampe, A.K., Richter, A., Tranvik, L.J., 2009. The boundless carbon cycle. Nat. Geosci. 2, 598–601.

De Alba, S., Borselli, L., Torri, D., Pellegrini, S., Bazzoffi, P., 2006. Assessment of tillage erosion by mouldboard plough in Tuscany (Italy). Soil Tillage Res. 85 (1–2), 123–142.

De Alba, S., Lindstrom, M., Schumacher, T.E., 2004. Soil landscape evolution due to soil redistribution by tillage: a new conceptual model of soil catena evolution in agricultural landscapes. Catena 58, 77–100.

Deumlich, D., Dannowski, R., Völker, L., 2014. Historische und aktuelle Geoinformation - Grundlage in der Agarlandschaftsforschung, *Zeitschrift für Geodäsie*. Geoinformation und Landmanagement 139, 329–341.

Dlugoß, V., Fiener, P., Van Oost, K., Schneider, K., 2012. Model based analysis of lateral and vertical soil C fluxes induced by soil redistribution processes in a small agricultural watershed. Earth Surf. Process. Landf. 37 (2), 193–208.

Doetterl, S., Berhe, A.A., Nadeu, E., Wang, Z., Sommer, M., Fiener, P., 2016. Erosion, deposition and soil carbon: a review on process-level controls, experimental tools and models to address C cycling in dynamic landscapes. Earth-Sci. Rev. 154, 102–122.

Dupin, B., de Rouw, A., Phantahvong, K.B., Valentin, C., 2009. Assessment of tillage erosion rates on steep slopes in northern Laos. Soil Tillage Res. 103 (1), 119–126.

Eltner, A., Baumgart, P., 2015. Accuracy constraints of terrestrial Lidar data for soil erosion measurement: application to a Mediterranean field plot. Geomorphology 245, 243–254.

Eltner, A., Baumgart, P., Maas, H.G., Faust, D., 2015. Multi-temporal UAV data for automatic measurement of rill and interrill erosion on loess soil. Earth Surf. Process. Landf. 40 (6), 741–755.

Fiener, P., Dlugoß, V., Van Oost, K., 2015. Erosion-induced carbon redistribution, burial and mineralisation - is the episodic nature of erosion processes important? Catena 133, 282–292.

Gerke, H.H., Koszinski, S., Kalettka, T., Sommer, M., 2010. Structures and hydrologic function of soil landscapes with kettle holes using an integrated hydropedological approach. J. Hydrol. 393 (1–2), 123–132.

Gifford, R.M., Roderick, M.L., 2003. Soil carbon stocks and bulk density: spatial or cumulative mass coordinates as a basis of expression? Glob. Chang. Biol. 9 (11), 1507–1514.

Govers, G., Lobb, D.A., Quine, T.A., 1999. Preface - tillage erosion and translocation: emergence of a new paradigm in soil erosion research. Soil Tillage Res. 51 (3–4), 167–174.

Govers, G., Quine, T.A., Desmet, P.J.J., Walling, D.E., 1996. The relative contribution of soil tillage and overland flow erosion to soil redistribution on agricultural land. Earth Surf. Process. Landf. 21, 929–946.

Govers, G., Quine, T.A., Walling, D.E., 1993. The effect of water erosion and tillage movement on hillslope profile development: a comparison of field observation and model results. In: Wicherek, S. (Ed.), Farm Land Erosion in Temperate Plains Environments and Hills. Elsevier, Amsterdam, pp. 285–300.

Govers, G., Vandaele, K., Desmet, P., Poesen, J., Bunte, K., 1994. The role of tillage in soil redistribution on hillslopes. Eur. J. Soil Sci. 45, 469–478.

Guzmán, G., Barrón, V., Gómez, J.A., 2010. Evaluation of magnetic iron oxides as sediment tracers in water erosion experiments. Catena 82 (2), 126–133.

Guzmán, G., Laguna, A., Cañasveras, J.C., Boulal, H., Barrón, V., Gómez-Macpherson, H., Giráldez, J.V., Gómez, J.A., 2015. Study of sediment movement in an irrigated maize-cotton system combining rainfall simulations, sediment tracers and soil erosion models. J. Hydrol. 524, 227–242.

Guzmán, G., Vanderlinden, K., Giráldez, J.V., Gómez, J.A., 2013. Assessment of spatial variability in water erosion rates in an olive orchard at plot scale using a magnetic iron oxide tracer. Soil Sci. Soc. Am. J. 77 (2), 350–361.

Hardy, R.A., Pates, J.M., Quinton, J.N., Coogan, M.P., 2016. A novel fluorescent tracer for real-time tracing of clay transport over soil surfaces. Catena 141, 39–45.

Heckrath, G., Djurhuus, J., Quine, T.A., Van Oost, K., Govers, G., Zhang, Y., 2005. Tillage erosion and its effect on soil properties and crop yield in Denmark. J. Environ. Qual. 34 (1), 312–324.

Heckrath, G., Halekoh, U., Djurhuus, J., Govers, G., 2006. The effect of tillage direction on soil redistribution by mouldboard ploughing on complex slopes. Soil Tillage Res. 88 (1–2), 225–241.

IUSS, 2015. World reference base for soil resources 2014. Update 2015. International Soil Classification System for Naming Soils and Creating Legends for Soil Maps. World Soil Resources Reports No. 106. FAO, Rome.

Jordanova, D., Jordanova, N., Atanasova, A., Tsacheva, T., Petrov, P., 2011. Soil tillage erosion estimated by using magnetism of soils - a case study from Bulgaria. Environ. Monit. Assess. 183 (1–4), 381–394.

Kietzer, B., 2007. Soil Translocation by Tillage Erosion in Ground Moraine Landscapes of NE Germany. p. 147.

Kimaro, D.N., Deckers, J.A., Poesen, J., Kilasara, M., Msanya, B.M., 2005. Short and medium term assessment of tillage erosion in the Uluguru Mountains, Tanzania. Soil Tillage Res. 81 (1), 97–108.

Kosmas, C., Gerontidis, S., Marathianou, M., Detsis, B., Zafiriou, T., Muysen, W.N., Govers, G., Quine, T.A., Van Oost, K., 2001. The effects of tillage displaced soil on soil properties and wheat biomass. Soil Tillage Res. 58 (1–2), 31–44.

Li, Y., Frielinghaus, M., Govers, G., Van Oost, K., Bork, H.R., Friedland, E.M., Schäfer, H., 1999. Spatial and temporal variations of tillage erosion at a moraine catena in NE Germany. 2nd International Symposium on Tillage Erosion and Tillage Translocation, Leuven, p. 42.

Lindstrom, M.J., Nelson, W.W., Schumacher, T.E., Lemme, G.D., 1990. Soil movement by tillage as affected by slope. Soil Tillage Res. 17 (3), 255–264.

Lobb, D.A., Kachanoski, R.G., Miller, M.H., 1995. Tillage translocation and tillage erosion on shoulder slope landscape positions measured using CS-137 as a tracer. Can. J. Soil Sci. 75 (2), 211–218.

Lobb, D.A., Kachanoski, R.G., Miller, M.H., 1999. Tillage translocation and tillage erosion in the complex upland landscapes of southwestern Ontario, Canada. Soil Tillage Res. 51, 189–209.

Lobb, D.A., Quine, T.A., Govers, G., Heckrath, G.J., 2001. Comparison of methods used to calculate tillage translocation using plot-tracers. J. Soil Water Conserv. 56 (4), 321–328.
Logsdon, S.D., 2013. Depth dependence of chisel plow tillage erosion. Soil Tillage Res. 128, 119–124.
Montanarella, L., Pennock, D.J., McKenzie, N., Badraoui, M., Chude, V., Baptista, I., Mamo, T., Yemefack, M., Singh Aulakh, M., Yagi, K., Young Hong, S., Vijarnsorn, P., Zhang, G.L., Arrouays, D., Black, H., Krasilnikov, P., Sobocká, J., Alegre, J., Henriquez, C.R., de Lourdes Mendonça-Santos, M., Taboada, M., Espinosa-Victoria, D., AlShankiti, A., AlaviPanah, S.K., Elsheikh, E.A.E.M., Hempel, J., Camps Arbestain, M., Nachtergaele, F., Vargas, R., 2016. World's soils are under threat. Soil 2 (1), 79–82.
d'Oleire-Oltmanns, S., Marzolff, I., Peter, K.D., Ries, J.B., 2012. Unmanned aerial vehicle (UAV) for monitoring soil erosion in Morocco. Remote Sens. 4 (11), 3390–3416.
Peter, K.D., d'Oleire-Oltmanns, S., Ries, J.B., Marzolff, I., Hssaine, A.A., 2014. Soil erosion in gully catchments affected by land-levelling measures in the Souss Basin, Morocco, analysed by rainfall simulation and UAV remote sensing data. Catena 113, 24–40.
Pimentel, D., 2006. Soil erosion: a food and environmental threat. Environ. Dev. Sustain. 8, 119–137.
Pimentel, D., Burgess, M., 2013. Soil erosion threatens food production. Agriculture 443–463.
Pineux, N., Lisein, J., Swerts, G., Bielders, C.L., Lejeune, P., Colinet, G., Degre, A., 2017. Can DEM time series produced by UAV be used to quantify diffuse erosion in an agricultural watershed? Geomorphology 280, 122–136.
Quine, T.A., Desmet, P.J.J., Govers, G., Vandaele, K., Walling, D.E., 1994. A comparison of the roles of tillage and water erosion in landform development and sediment export on agricultural land near Leuven, Belgium. IAHS Publ. 224, 77–86.
Quine, T.A., Walling, D.E., Govers, G., 1996. Simulation of radiocaesium redistribution on cultivated hillslopes using a mass-balance model: an aid to process interpretation and erosion rate estimation. In: Anderson, M.G., Brooks, S.M. (Eds.), Advances in Hillslope Processes. Wiley & Sons, Chichester, pp. 561–588.
Quine, T.A., Zhang, Y., 2004. Re-defining tillage erosion: quantifying intensity-direction relationships for complex terrain. 2. Revised mouldboard erosion model. Soil Use Manag. 20 (2), 124–132.
Quinton, J.N., Govers, G., Van Oost, K., Bardgett, R.D., 2010. The impact of agricultural soil erosion on biogeochemical cycling. Nat. Geosci. 3, 311–314.
Sadowski, H., Sorge, B., 2005. Der Normalhöhenpunkt von 1912 - Datumspunkt des DHHN 2012? Vermessung Brandenburg 2 (2005), 31–39.
Sommer, M., Gerke, H.H., Deumlich, D., 2008. Modelling soil landscape genesis — a "time split" approach for hummocky agricultural landscapes. Geoderma 145 (3–4), 480–493.
Thapa, B.B., Cassel, D.K., Garrity, D.P., 1999. Assessment of tillage erosion rates on steepland Oxisols in the humid tropics using granite rocks. Soil Tillage Res. 51 (3–4), 233–243.
Tiessen, K.H.D., Mehuys, G.R., Lobb, D.A., Rees, H.W., 2007. Tillage erosion within potato production systems in Atlantic Canada - I. Measurement of tillage translocation by implements used in seedbed preparation. Soil Tillage Res. 95 (1–2), 308–319.
Tranvik, L.J., Downing, J.A., Cotner, J.B., Loiselle, S.A., Striegl, R.G., Ballatore, T.J., Dillon, P., Finlay, K., Fortino, K., Knoll, L.B., Kortelainen, P.L., Kutser, T., Larsen, S., Laurion, I., Leech, D.M., McCallister, S.L., McKnight, D.M., Melack, J.M., Overholt, E., Porter, J.A., Prairie, Y., Renwick, W.H., Roland, F., Sherman, B.S., Schindler, D.W., Sobek, S., Tremblay, A., Vanni, M.J., Verschoor, A.M., Von Wachenfeldt, E., Weyhenmeyer, G.A., 2009. Lakes and reservoirs as regulators of carbon cycling and climate. Limnol. Oceanogr. 54 (6), 2298–2314.
Turkelboom, F., Poesen, J., Ohler, I., VanKeer, K., Ongprasert, S., Vlassak, K., 1997. Assessment of tillage erosion rates on steep slopes in northern Thailand. Catena 29 (1), 29–44.
Van Muysen, W., Govers, G., 2002. Soil displacement and tillage erosion during secondary tillage operations: the case of rotary harrow and seeding equipment. Soil Tillage Res. 65 (2), 185–191.
Van Muysen, W., Govers, G., Van Oost, K., 2002. Identification of important factors in the process of tillage erosion: the case of mouldboard tillage. Soil Tillage Res. 65 (1), 77–93.
Van Muysen, W., Govers, G., Van Oost, K., Van Rompaey, A., 2000. The effect of tillage depth, tillage speed, and soil condition on chisel tillage erosivity. J. Soil Water Conserv. 55 (3), 2–11.
Van Oost, K., Govers, G., 2006. Tillage erosion. In: Boardman, J., Poesen, J. (Eds.), Soil erosion in Europe. Wiley, Chichester, pp. 599–608.
Van Oost, K., Govers, G., De Alba, S., Quine, T.A., 2006. Tillage erosion: a review of controlling factors and implications for soil quality. Prog. Phys. Geogr. 30, 443–466.
Van Oost, K., Govers, G., Desmet, P., 2000. Evaluating the effects of changes in landscape structure on soil erosion by water and tillage. Landsc. Ecol. 15, 577–589.
Van Oost, K., Govers, G., Quine, T., Heckarth, G., Olesen, J.E., De Gryze, S., Merckx, R., 2005. Landscape-scale modeling of carbon cycling under the impact of soil redistribution: the role of tillage erosion. Glob. Biogeochem. Cycles 19 (4), 1–13.
Van Oost, K., Govers, G., Van Muysen, W., 2003. A process-based conversion model for caesium-137 derived erosion rates on agricultural land: an integrated spatial approach. Earth Surf. Process. Landf. 28 (2), 187–207.
Van Oost, K., Govers, G., Van Muysen, W., Quine, T.A., 2000. Modelling translocation and dispersion of soil constituents by tillage on sloping land. Soil Sci. Soc. Am. J. 64 (5), 1733–1739.
Van Oost, K., Quine, T., Govers, G., Heckrath, G., 2005. Modeling soil erosion induced carbon fluxes between soil and atmosphere on agricultural land using SPEROS-C. In: Roose, E.J., Lal, R., Feller, C., Barthes, B., Stewart, B.A. (Eds.), Advances in Soil Science. Soil Erosion and Carbon Dynamics. CRC Press, Boca Raton, pp. 37–51.
Van Rompaey, A.J.J., Verstraeten, G., Van Oost, K., Govers, G., Poesen, J., 2001. Modelling mean annual sediment yield using a distributed approach. Earth Surf. Process. Landf. 26 (11), 1221–1236.
Vandaele, K., Vanommeslaeghe, J., Muylaert, R., Govers, G., 1996. Monitoring soil redistribution patterns using sequential aerial photographs. Earth Surf. Process. Landf. 21, 353–364.
Vanwalleghem, T., Jimenez-Hornero, F.J., Giraldez, J.V., Laguna, A., 2010. Simulation of long-term soil redistribution by tillage using a cellular automata model. Earth Surf. Process. Landf. 35 (7), 761–770.
Vieira, D.A.N., Dabney, S.M., 2011. Modeling edge effects of tillage erosion. Soil Tillage Res. 111 (2), 197–207.
Vinci, A., Brigante, R., Todisco, F., Mannocchi, F., Radicioni, F., 2015. Measuring rill erosion by laser scanning. Catena 124, 97–108.
Wilken, F., Sommer, M., Van Oost, K., Bens, O., Fiener, P., 2017. Process-oriented modelling to identify main drivers of erosion-induced carbon fluxes. Soil 3 (2), 83–94.
Zhang, J.H., Li, F.C., 2011. An appraisal of two tracer methods for estimating tillage erosion rates under hoeing tillage. Environ. Eng. Manag. J. 10 (6), 825–829.